DESIGN OF AN XUV FEL DRIVEN BY THE LASER-PLASMA ACCELERATOR AT THE LBNL LOASIS FACILITY[*]

C. B. Schroeder, W. M. Fawley, E. Esarey, W. P. Leemans
Lawrence Berkeley National Laboratory, Berkeley, CA 94720, USA

Abstract

We present a design for a compact FEL source of ultra-fast, high-peak flux, soft x-ray pulses employing a high-current, GeV-energy electron beam from the existing laser-plasma accelerator at the LBNL LOASIS laser facility. The proposed ultra-fast source would be intrinsically temporally synchronized to the drive laser pulse, enabling pump-probe studies in ultra-fast science with pulse lengths of tens of fs. Owing both to the high current ($\sim$10 kA) and reasonable charge/pulse ($\sim$0.1–0.5 nC) of the laser-plasma-accelerated electron beams, saturated output fluxes are potentially $10^{13} - -10^{14}$ photons/pulse. We examine devices based both on SASE and high-harmonic generated input seeds to give improved coherence and reduced undulator length, presenting both analytic scalings and numerical simulation results for expected FEL performance. A successful source would result in a new class of compact laser-driven FELs in which a conventional RF accelerator is replaced by a GeV-class laser-plasma accelerator whose active acceleration region is only a few cm in length.

INTRODUCTION

Recent advances in laser-plasma-based accelerators have demonstrated generation of low energy spread, $\sim$100 MeV electron beams [1]. These experiments used an ultra-intense $\sim$$10^{19}$ W/cm^2 laser pulse focused on a gas jet, with typical length of a few millimeters, to generate plasma waves with accelerating fields on the order of 100 GV/m. By using a gas-filled discharge capillary for creating a plasma channel, the laser-plasma interaction length can be extended to a few centimeters, resulting in high-quality GeV electron beams [2]. In addition, the electron bunches emerging from a laser-plasma accelerator have naturally short durations (tens of fs) [3], and are intrinsically synchronized to the short-pulse laser driver, making such a source ideal for ultra-fast pump-probe applications. These laser-plasma accelerator experimental results [1, 2] open the possibility of a new class of compact, high-peak flux, x-ray free-electron laser (FEL) in which the conventional radio-frequency (RF) accelerator (10–100 m length) is replaced by a GeV-class laser-plasma accelerator (several cm length), in principle greatly reducing the size and cost of such light sources [4].

In this paper we discuss the design of an XUV FEL driven by the existing laser-plasma accelerator at the LOA-

SIS laser facility at LBNL.

LASER-PLASMA ACCELERATOR

The LOASIS Laboratory at LBNL presently produces ultra-short ($<$50 fs), relativistic electron bunches with high charge ($\gtrsim$100 pC/bunch) via a laser-plasma interaction. The bunches are generated by a laser wakefield accelerator (LWFA): radiation pressure from a short pulse, intense laser excites high-field plasma waves (wakefields) that accelerate electrons [5]. The LWFA at LBNL uses a 10 Hz, Ti:Sapphire laser system to focus ultra-short ($\sim$30 fs) laser pulses of relativistic intensity ($>$$10^{18}$ W/cm^2) into a plasma channel. GeV-energy electron beams have been demonstrated [2] using the LBNL 100 TW-class laser system and a gas-filled capillary discharge waveguide [6] for plasma channel production, which allows for low plasma densities ($\sim$$10^{18}$ cm^{-3}) and long ($\sim$cm) laser-plasma interaction lengths. These LWFA-produced electron beams are high current ($\sim$10 kA) and ultra-short ($<$50 fs), properties which are attractive as an input beam for an FEL generating ultra-short x-rays.

In recent experiments using the plasma-channel-guided LWFA at LBNL, a 18-TW, 72-fs laser (25 μm focused spot size) is guided in capillary waveguide (which generates a plasma channel via a discharge in the hydrogen filled capillary), producing 0.5 GeV with 5% RMS *projected* relative energy spread, 2.0 mrad RMS divergence, and 50 pC of charge [2]. Experimental results using 2 J of laser energy have produced 1-nC electron beams at 0.5 GeV. At present, *slice* energy spread σ_γ measurements of the electron beam have not been performed, but simulation results [7] predict that the slice energy spread is an order of magnitude smaller than the projected value.

FEL DESIGN

We consider interaction of the LWFA-generated 0.5-GeV electron beam in a conventional magnetostatic undulator. For this study we will consider the LWFA electron beam and undulator parameters listed in Table 1; the latter correspond to the existing "THUNDER" device (see Ref. [8] for a detailed description), which provisionally will be transferred to LBNL from Boeing in late 2006. THUNDER contains 220 periods divided into ten 50-cm sections, each separated by a 4-cm diagnostic and steering space. The maximum RMS undulator strength parameter is $a_u = K/\sqrt{2} \simeq 1.31$ ($\approx$1.0 T peak magnetic field) which may be tapered section by section. Wiggle-plane

focusing is provided by a canted pole configuration with the expected matched beta-function $k_\beta^{-1} \approx 3.6\,\text{m}$ for the peak field and 0.5-GeV beam. Conventional magnetic optics will transport the electron beam from the laser-plasma accelerator to the undulator. Note that there could be nontrivial beam transport issues concerning the required degree of achromaticity and preservation of pulse duration (*i.e.*, peak current). At 0.5 GeV, the beam is sufficiently "stiff" that pulse lengthening via drift will be small; for example, a 5% energy chirp results in less than 1 fs of pulse lengthening over a transport distance of a few meters.

Table 1: Electron Beam, Undulator and HHG Source Parameters

LWFA electron beam:	
Beam energy, γmc^2	0.5 GeV
Peak current, I	5 kA
Charge, Q	0.1 nC
Bunch duration (FWHM), τ_b	20 fs
Energy spread (RMS, slice), σ_γ/γ	0.25%
Normalized transverse emittance	1 mm mrad
Undulator:	
Undulator type	planar
Undulator period, λ_u	2.18 cm
Peak magnetic field	1.02 T
Undulator parameter (peak), K	1.85
Magnetic gap	4.8 mm
Beta-function, k_β^{-1}	3.6 m
HHG seed:	
HHG radiation wavelength	31 nm
Coherent HHG radiation power	15 MW
HHG pulse duration	20 fs

FEL PERFORMANCE

We consider two modes of FEL operation: self-amplified spontaneous emission (SASE) and seeding by a high-harmonic generation (HHG) source. Results from FLASH at DESY [9] and SSCS at Spring-8 [10], operating in the XUV wavelength regime, have confirmed the applicability of the basic SASE physics at XUV wavelengths. Existing laboratory HHG sources have demonstrated production of ultra-short (tens of fs) coherent soft x-ray (*e.g.,* 31 nm, 26th harmonic of a 0.8 μm drive laser) pulses with 0.3 μJ of energy (see, *e.g.,* Ref. [11]). HHG seeding has significant advantages over the simpler SASE mode of operation as it will provide improved temporal coherence and a much reduced power saturation length.

The resonant wavelength for the beam and undulator parameters of Table 1 is $\lambda = \lambda_u(1 + K^2/2)/(2\gamma^2) \simeq$ 31 nm (40-eV photons), while the matched electron beam size in the undulator is 60 μm. The FEL parameter is $\rho \approx 5 \times 10^{-3}$ and the ideal 1D (*i.e.*, no emittance, energy spread, or diffraction effects) exponential power gain
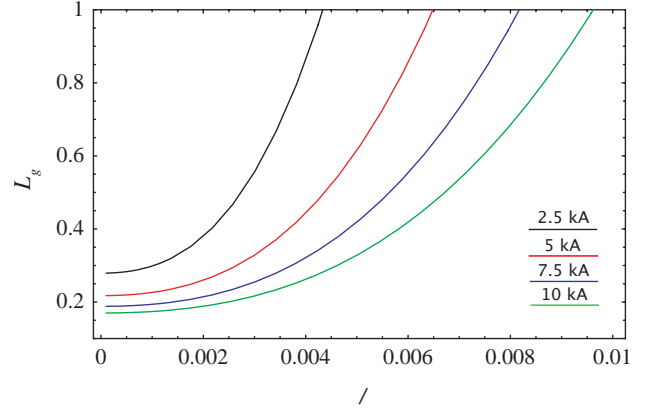

Figure 1: Exponential gain length as a function of incoherent energy spread for various electron beam currents as determined from the Xie [12] empirical fitting function.

length is $L_{1D} = \lambda_u/(4\pi\sqrt{3}\rho) \simeq 0.19\,\text{m}$. Including these non-ideal effects via the Xie gain length formula [12] can increase the gain length (L_g) 1.5–3 fold compared to the ideal 1D gain length, depending upon the assumed value of σ_γ. For the parameters of Table 1, the 3D gain length is $L_g \approx 0.3\,\text{m}$. Figure 1 displays contours of gain length as a function of peak current I and relative energy spread σ_γ/γ. If one presumes empirically that the product $I\sigma_\gamma$ remains constant, one sees that it is best to operate at relatively large currents. However, consideration of slippage effects over the full THUNDER undulator ($\tau_s = \lambda N_u/c \approx 24$ fs) suggests that reducing the electron beam pulse duration τ_b below τ_s will have diminishing returns. Hence, we believe peak currents of $I \sim 2.5$–10 kA for a bunch charge of $Q \approx 100$ pC is the likely region of interest. Space charge effects will not degrade the FEL performance in this high-current regime provided $(\lambda_u/\lambda_p)^2/\gamma^3 \ll (2\rho)^2$ (*i.e.*, the characteristic wavelength of the space charge oscillation in the lab frame is much greater than the FEL gain length), where λ_p is the plasma wavelength of the electron beam. This condition is satisfied for the parameters of Table 1.

We performed a series of time-independent GINGER [13] simulations to examine in detail the predicted FEL output from such a device, examining both the SASE and HHG-seeded cases. We adopted electron beam and undulator parameters as given in Table 1 with the exception that we also considered 7.5-kA peak current (150 pC charge) SASE and HHG-seeded cases and a 10-kA peak current (200 pC charge) SASE case, in addition to the nominal 5-kA HHG-seeded FEL. The simulations used a parabolic temporal profile for the electron beam; the details (*i.e.*, the sub-20 fs structure) of the actual experimental electron beam profile have not been measured. All the SASE results presented here are from one single simulation run for each of the two currents. Note that an ensemble average over many different runs, each with a different initial shot noise presentation would give smoother profiles for $P(t)$ and $P(\omega)$.

Figure 2 shows the maximum power for the HHG-seeded case (FEL in amplifier mode with 15 MW initial HHG
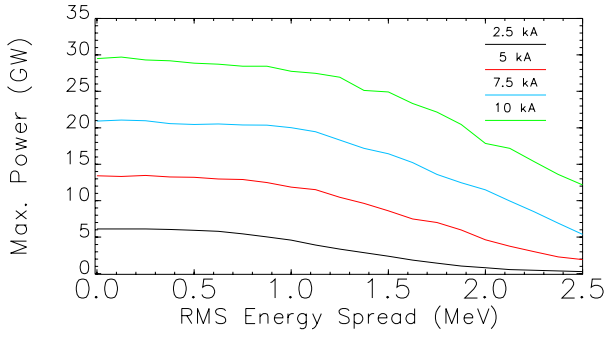
Figure 2: Predicted (GINGER calculations) maximum power in amplifier mode (with 15 MW initial HHG seed) over the THUNDER undulator (5 m) as a function of initial incoherent energy spread for various beam currents.
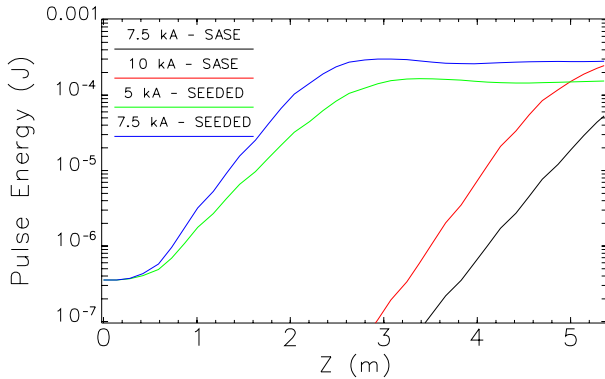

Figure 3: Predicted (GINGER calculations) radiation pulse energies as a function of undulator length z for both SASE and HHG-seeded cases.
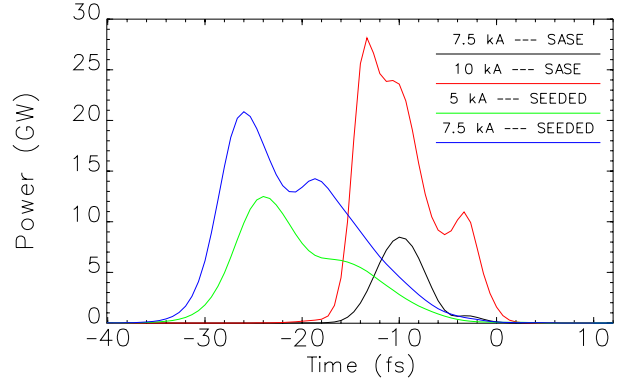

Figure 4: Predicted (GINGER calculations) output power temporal profiles for the cases associated with Fig. 3. The electron beam center is at $t = 0$.
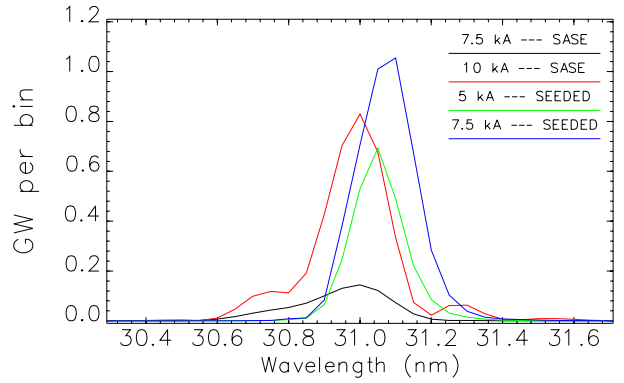

Figure 5: Predicted (GINGER calculations) output spectra at the 31-nm wavelength fundamental for the various SASE and seeded cases. Each bin is 64.6 meV wide while 1 GW is equivalent to 1.0×10^{13} photons.

seed) versus initial incoherent RMS energy spread for several beam currents. As the figure shows, for the nominal beam current (5 kA), greater than 10 GW of power can be achieved provided the RMS energy spread is $\lesssim 1.25$ MeV ($\sigma_\gamma/\gamma \lesssim 0.25\%$).

Figure 3 displays time-integrated radiation pulse energies as a function of undulator length z; for reference, 1 μJ of energy corresponds to 1.5×10^{11} photons at 40 eV. The SASE results show a strong current dependence that is attributable to the sensitivity of L_g to current in this short-pulse regime with normalized σ_γ comparable to ρ. One sees in Fig. 3 that the 7.5-kA SASE case is about a gain length away from saturation, while the 10-kA SASE case reaches saturation. Given that we presumed idealized Gaussian transverse distributions with no offsets, tilts, *etc.*, additional current and charge might be required to reach full saturation with the assumed energy spread of 1.25 MeV. Earlier saturation in z might also be achieved by employing additional focusing (by adding focusing optics between the THUNDER undulator sections) thereby reducing the beta-function. Saturation is achieved in <3-m distance for the HHG-seeded cases.

Figure 4 shows output power temporal radiation profiles; one sees that the radiation pulse remains temporally close to the electron beam (whose center is at $t = 0$) when com-

pared with slippage ($\tau_s \approx 24$ fs). Since the electron beam duration τ_b is only a few times the steady-state coherence length $c\tau_c \equiv \lambda/(4\pi\rho_{3D})$, the output profile is dominated by a single longitudinal mode, which results in spectral purity (at the price of reduced gain). This is apparent also in Fig 5 which shows quite clean power spectra for all cases except the 10-kA SASE run where there appear to be weak "sidebands" to either side of the central line; we expect ensemble average over many shots would likely show a simple Gaussian shape whose width would be slightly wider than this specfic run.

For the HHG-seeded cases shown in Figs. 3, 4, and 5 we presumed an input seed with a 20-fs FWHM Gaussian temporal profile and peak power of 15 MW. The results indicate significantly improved performance of the HHG-seeded FEL, compared to the SASE cases (*e.g.,* compare the 7.5-kA cases). As seen in Fig. 3, saturation occurs before 3 m in the undulator, and peak powers exceeding 10 GW appear possible with FWHM durations ~15 fs (Fig. 4). Despite the early saturation, both HHG-seeded cases (5 kA and 7.5 kA) show essentially single mode spectral output with inverse normalized bandwidths (RMS) for the on-axis far field of $\omega/\Delta\omega \approx 500$ and autocorrelation times $\sim$ 12 fs. Predicted third harmonic power (due to

Table 2: FEL Performance

Radiation wavelength, λ	31 nm
Resonant photon energy	40 eV
FEL parameter, ρ	5×10^{-3}
3D Gain length	0.3 m
Slippage length	7.2 μm
Spontaneous radiation power	4 kW
Steady-state saturation power	12 GW
Photon/pulse (at saturation)	3×10^{13}
Peak brightness[a] (at saturation)	2×10^{16}
Saturation length (HHG-seeded, 5 kA)	2.4 m
Saturation length (SASE, 10 kA)	5 m

[a] photons/pulse/mm^2/mrad^2/0.1% BW

the nonlinear harmonic microbunching associated with the strong fundamental bunching) is about 0.4% and 0.8% of the fundamental for the 5-kA and 7.5-kA cases, respectively. The normalized spectral bandwidths for the third harmonic are narrower than the fundamental by slightly more than a factor of two; one expects less than the theoretical maximum of three due to the variation in temporal microbunching fraction [*i.e.,* the third-harmonic bunching parameter $b_3(t)$ has a narrower pulse shape than the fundamental $b_1(t)$]. Despite the much lower photon/pulse value of the third harmonic radiation, it may, nonetheless, be of interest for certain experiments.

DISCUSSION AND CONCLUSIONS

Recent advances in laser-plasma-based accelerator experiments [1, 2], and, in particular, the demonstration of high quality GeV electron beams [2], have enabled the possibility of a new class of compact laser-driven FELs in which the conventional RF accelerator is replaced by a cm-scale laser-plasma accelerator, greatly reducing the size and cost of the FEL. The natural short bunch length of the laser-plasma accelerator (tens of fs), and the intrinsic temporal synchronization between the short-pulse laser generating the electron beam and the FEL radiation, make the laser-driven FEL an ideal source for ultra-fast pump-probe applications. As discussed above, seeding of the FEL by an HHG source (generated from the same LWFA drive laser, and, therefore, temporally synchronized with the electron beam) has significant advantages over the simpler SASE mode of operation. The coherent amplification of the HHG source in the FEL leads to reduced undulator length and improved longitudinal coherence.

In this paper we have discussed the design of a XUV FEL employing the 0.5 GeV laser-plasma-generated electron beam produced at the LOASIS laser facility at LBNL. Table 2 shows the expected FEL performance employing a 31-nm HHG seed assuming the input parameters given in Table 1. Presuming a reasonably small incoherent energy spread of 1.25 MeV, a 15 MW HHG input seed pro-

vides sufficient initial power for the FEL to reach saturation in a few meters using the THUNDER undulator. For SASE, higher currents (*e.g.,* 10 kA) are needed to reach saturation in the 5 m undulator distance. The proposed HHG-seeded FEL, using the existing 0.5 GeV-LWFA at LBNL and the THUNDER undulator would capable of producing ultra-short ($\sim$15 fs) XUV (40 eV) pulses with $>10^{13}$ photons/pulse. The predicted third harmonic emission would be $\sim$ 2.5 orders of magnitude less. A key beam parameter is the actual incoherent (*i.e.,* slice) energy spread. Values much above 1.25 MeV (0.25%) would require peak currents $\geq$ 10 kA for saturation to occur within the THUNDER undulator.

REFERENCES

[1] S. P. D. Mangles *et al.*, Nature 431 (2004) 535; C. G. R. Geddes *et al.*, *ibid.* 431 (2004) 538; J. Faure *et al.*, *ibid.* 431 (2004) 541.

[2] W. P. Leemans *et al.*, Nature Phys. (2006) in press.

[3] J. van Tilborg *et al.*, Phys. Rev. Lett. 96 (2006) 014801.

[4] D. A. Jaroszynski *et al.*, Phil. Trans. R. Soc. A 364 (2006) 689.

[5] E. Esarey *et al.*, IEEE Trans. Plasma Sci. 24 (1996) 252.

[6] D. J. Spence and S. M. Hooker, Phys. Rev. E 63 (2001) 015401.

[7] C. G. R. Geddes *et al.*, Phys. Plasmas 12 (2005) 056709.

[8] K. E. Robinson, D. C. Quimby and J. M. Slater, IEEE J. Quantum Electron. QE-23, (1987) 1497.

[9] V. Ayvazyan *et al.*, Eur. Phys. J. D 37 (2006) 297.

[10] T. Shintake, "First Lasing at SCSS", Paper MOAAU04, these proceedings.

[11] E. Takahashi *et al.*, Phys. Rev. E 66 (2002) 021802(R).

[12] M. Xie, Nucl. Instrum. Methods Phys. Res. A445 (2000) 59.

[13] W. M. Fawley, LBNL Technical Report No. LBNL-49625 (2002); see also paper MOPPH073, these proceedings.